Hindawi Publishing Corporation
Mathematical Problems in Engineering
Volume 2013, Article ID 359817, 12 pages
http://dx.doi.org/10.1155/2013/359817

Research Article

MHD Slip Flow of Newtonian Fluid past a Stretching Sheet with Thermal Convective Boundary Condition, Radiation, and Chemical Reaction

Reda G. Abdel-Rahman

Mathematics Department, Faculty of Science, Benha University, Benha 13518, Egypt

Correspondence should be addressed to Reda G. Abdel-Rahman; redakhaled2004@yahoo.com

Received 8 June 2013; Accepted 23 July 2013

Academic Editor: Mohamed Abd El Aziz

An analysis is carried out to study the problem of heat and mass transfer flow over a moving permeable flat stretching sheet in the presence of convective boundary condition, slip, radiation, heat generation/absorption, and first-order chemical reaction. The viscosity of fluid is assumed to vary linearly with temperature. Also the diffusivity is assumed to vary linearly with concentration. The governing partial differential equations have been reduced to the coupled nonlinear ordinary differential equations by using Lie group point of transformations. The system of transformed nonlinear ordinary differential equations is solved numerically using shooting techniques with fourth-order Runge-Kutta integration scheme. Comparison between the existing literature and the present study was carried out and found to be in excellent agreement. The effects of the various interesting parameters on the flow, heat, and mass transfer are analyzed and discussed through graphs in detail. The values of the local Nusselt number, the local skin friction, and the local Sherwood number for different physical parameters are also tabulated.

1. Introduction

Investigations of laminar boundary flow of an electrically conducting fluid over a moving continuous stretching surface are important in many manufacturing processes, such as materials manufactured by polymer extrusion, continuous stretching of plastic films, artificial fibers, hot rolling, wire drawing, glass fiber, metal extrusion and metal spinning, cooling of metallic sheets, or electronic chips. The first and foremost work regarding the boundary-layer behavior in moving surfaces in quiescent fluid was considered by Sakiadis [1]. Heat and mass transfers on stretched surface with suction and injection was introduced by Fox et al. [2]. P. S. Gupta and A. S. Gupta [3] studied the same problem for linearly stretching sheet. Heat transfer past a moving continuous plate with variable temperature was studied by Soundalgekar and Murty [4] and Grubka and Bobba [5]. Subsequently, many researchers [6–12] worked on the problem of moving or stretching plates under different situations.

MHD viscous flow over a stretching sheet in the presence of slip velocity was studied by many authors, such as Martin and Boyd [13], Fang and Lee [14], Ariel et al. [15], Andersson [16], Wang [17, 18], Mukhopadhyay and Anderson [19], Fang [20], and Hayat et al. [21]. Fang et al. [22] studied MHD viscous flow over a permeable shrinking sheet. They observed that the velocity at the wall increased with slip parameter. Mahmoud and Waheed [23] included the effects of slip and heat generation/absorption on MHD mixed convection flow of a micropolar fluid over a heated stretching surface. Recently, Hamad et al. [24] investigated heat and mass transfer over a moving porous plate with hydrodynamic slip and thermal convective boundary conditions. They found that the wall slip velocity and wall shear stress are a decreasing function of the slip parameter.

Thermal radiation effects on an electrically conducting fluid arise in many practical applications such as electrical power generation, solar power technology, nuclear reactors, and nuclear waste disposal (see Mahmoud [25] and Chamkha

[26]). Radiation effects on boundary layer flow with and without applying a magnetic field have been investigated by many authors [27–33] under certain conditions.

Heat and mass transfer problems with a chemical reaction have received a considerable amount of attention due to their importance in many chemical engineering processes, for example, food processing, manufacturing of ceramics, and polymer production. On the other hand, the study of heat generation or absorption in moving fluids is important in problems dealing with chemical reactions and those concerned with dissociating fluids. Possible heat generation effects may alter the temperature distribution and, consequently, the particle deposition rate in nuclear reactors, electronic chip, and semiconductor wafers. Many investigators [34–40] displayed the effects of heat generation and chemical reactions on heat transfer over a stretching sheet under various conditions. Recently, thermal convective surface boundary conditions were used by several authors such as Ishak [41], Makinde [42], Yao et al. [43], Hamad et al. [24], and Ferdows et al. [44].

Lie group point of transformations can be used to generate similarity transformations. It reduces the number of independent variables of the partial differential equations and keeps the system and associated initial and boundary conditions invariant. Reviews for the mathematical theory and applications of Lie group point of transformations to differential equations may be found in the texts by Olver [45], Bluman and Kumei [46], Hill [47], and Ibragimov and Kovalev [48]. This technique has been applied by many researchers to solve different flow phenomena over different geometries (see [49–52]).

Motivated by the previous works, the aim of the present work is to study the problem of heat and mass of Newtonian fluid with thermal convective boundary condition, slip velocity, radiation, heat generation/absorption, and first-order chemical reaction taking into account the viscosity dependent on the temperature and the thermal diffusivity dependent on the concentration. This problem has not been studied before despite its applications in many engineering processes, such as nuclear waste, polymer production, dispersion of chemical pollutants through water-saturated soil, geothermal energy extractions, plasma studies, liquid metal fluids, and power generation systems.

2. Mathematical Formulation of the Problem

Consider laminar boundary layer flow heat and mass transfer of viscous incompressible Newtonian fluid over moving stretching sheet as shown in Figure 1. A magnetic field of nonuniform $B(\overline{x})$ is applied parallel to the $\overline{y}$ axis. The bottom surface of the plate is heated by convection from a hot fluid of temperature $\overline{T}_f$, and this generates a heat transfer coefficient $h_f(\overline{x})$, and $\overline{T}_\infty$ is the ambient fluid temperature. The mass concentration of the species at the plate is also maintained uniform $\overline{C}_w$ which is also higher than the ambient fluid concentration $\overline{C}_\infty$. Figure 1 shows the coordinates and flow model. Under these assumptions and boundary layer

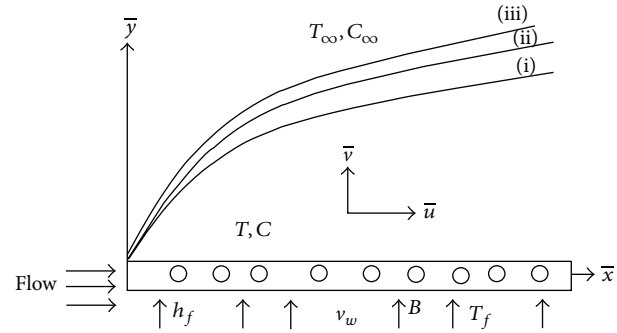

(i) Concentration
(ii) Thermal
(iii) Momentum B.L

Figure 1: Flow configuration.

approximations, the governing equations are

$$\frac{\partial \overline{u}}{\partial \overline{x}} + \frac{\partial \overline{v}}{\partial \overline{y}} = 0, \tag{1}$$

$$\overline{u}\frac{\partial \overline{u}}{\partial \overline{x}} + \overline{v}\frac{\partial \overline{u}}{\partial \overline{y}} = \frac{1}{\rho}\frac{\partial}{\partial \overline{y}}\left(\mu\left(\overline{T}\right)\frac{\partial \overline{u}}{\partial \overline{y}}\right) - \frac{\sigma_0}{\rho}B_0^2(\overline{x})\,\overline{u}, \tag{2}$$

$$\overline{u}\frac{\partial \overline{T}}{\partial \overline{x}} + \overline{v}\frac{\partial \overline{T}}{\partial \overline{y}} = \frac{\kappa}{\rho c_p}\frac{\partial^2 \overline{T}}{\partial \overline{y}^2} - \frac{1}{\rho c_p}\frac{\partial q_r}{\partial \overline{y}} + \frac{Q_0(\overline{x})}{\rho c_p}\left(\overline{T} - \overline{T}_\infty\right), \tag{3}$$

$$\overline{u}\frac{\partial \overline{C}}{\partial \overline{x}} + \overline{v}\frac{\partial \overline{C}}{\partial \overline{y}} = \frac{\partial}{\partial \overline{y}}\left(D\left(\overline{C}\right)\frac{\partial \overline{C}}{\partial \overline{y}}\right) - K(\overline{x})\left(\overline{C} - C_\infty\right), \tag{4}$$

subject to the boundary conditions

$$\overline{u} = U_w(\overline{x}) + \lambda_0(\overline{x})\,\mu\left(\overline{T}\right)\frac{\partial \overline{u}}{\partial \overline{y}}, \qquad \overline{v} = V_w(\overline{x}),$$

$$\kappa\frac{\partial \overline{T}}{\partial y} = -h_f(\overline{x})\left[\overline{T}_f - \overline{T}(\overline{x})\right], \quad \overline{C} = \overline{C}_w, \quad \text{at } \overline{y} = 0,$$

$$\overline{u} \longrightarrow 0, \qquad \overline{T} \longrightarrow \overline{T}_\infty, \qquad \overline{C} \longrightarrow \overline{C}_\infty, \qquad \text{as } \overline{y} \longrightarrow \infty, \tag{5}$$

where $\overline{u}$ and $\overline{v}$ are the velocities in $\overline{x}$ (along the sheet) and $\overline{y}$ (normal to the sheet) directions, respectively, $V_w(\overline{x})$ is the mass transfer velocity, μ is the coefficient of dynamic viscosity, $\nu = (\mu/\rho)$ is the kinematic coefficient of viscosity, $D(\overline{C})$ is the variable diffusivity, σ_0 is the electric conductivity, ρ is the density of the fluid, c_p is the specific heat at constant pressure, κ is the thermal conductivity, $\lambda_0(\overline{x})$ is the velocity slip factor having dimension (velocity)$^{-1}$, $U_w(\overline{x})$ is the velocity of moving plate, $V_w(\overline{x})$ is the suction or injection velocity through the surface, $\overline{T}$ is the temperature, $\overline{C}$ is the species concentration, $K(\overline{x})$ is the rate of chemical reaction, and $Q_0(\overline{x})$ is the heat generation/absorption rate. The subscripts denote wall conditions and free stream conditions, respectively.

Using Rosseland approximation for radiation [53], we can write $q_r = -(4\sigma_1/3\kappa^*)(\partial\overline{T}^4/\partial\overline{y})$, where σ_1 is the Stefan-Boltzmann constant and κ^* is the mean absorption coefficient. Assuming that the temperature difference is within the flow such that $\overline{T}^4$ may be expanded in a Taylor series and expanding $\overline{T}^4$ about $\overline{T}_\infty$ and neglecting higher orders, we get $\overline{T}^4 \cong 4\overline{T}_\infty^3\overline{T} - 3\overline{T}_\infty^4$. Therefore, (3) becomes

$$\overline{u}\frac{\partial\overline{T}}{\partial\overline{x}} + \overline{v}\frac{\partial\overline{T}}{\partial\overline{y}} = \frac{\kappa}{\rho c_p}\frac{\partial^2\overline{T}}{\partial\overline{y}^2} + \frac{16\sigma_1\overline{T}_\infty^3}{3\kappa^*\rho c_p}\frac{\partial^2\overline{T}}{\partial\overline{y}^2} + Q_0(\overline{x})\left(\overline{T} - \overline{T}_\infty\right). \tag{6}$$

We assume that the temperature dependent viscosity is varying linearly and is given by (see [54])

$$\mu\left(\overline{T}\right) = \mu_\infty\left[a_0 + b_0\left(\overline{\overline{T}_f} - \overline{T}\right)\right], \tag{7}$$

where μ_∞ is the coefficient of viscosity far away from the plate and b_0 and a_0 are constants depend on the nature of the fluid. We choose $a_0 = 1$.

Also here, we assume that the concentration diffusivity varies linearly as (see [55])

$$D\left(\overline{C}\right) = D_m\left[1 + d\left(\overline{C} - \overline{C}_\infty\right)\right], \tag{8}$$

where D_m is the constant concentration diffusivity and d is a constant.

We introduce the nondimensional parameters

$$\begin{aligned} x &= \frac{\overline{x}}{L}, \qquad y = \frac{\overline{y}}{L}\sqrt{\mathrm{Re}}, \qquad u = \frac{\overline{u}}{U_0}, \\ v &= \frac{\overline{v}}{U_0}\sqrt{\mathrm{Re}}, \qquad U_w(x) = \frac{\overline{U}_w(\overline{x})}{U_0}, \\ V_w(x) &= \frac{\overline{V}_w(\overline{x})}{U_0}, \qquad \theta = \frac{\overline{T} - \overline{T}_\infty}{\overline{T}_f - \overline{T}_\infty}, \\ \phi &= \frac{\overline{C} - \overline{C}_\infty}{\overline{C}_w - \overline{C}_\infty}, \end{aligned} \tag{9}$$

with L being characteristic length, $\mathrm{Re} = LU_0/\nu$ is the Reynolds number, and U_0 is a reference velocity. Also, we introduce stream function ψ defined as

$$u = \frac{\partial\psi}{\partial y}, \qquad v = -\frac{\partial\psi}{\partial x}. \tag{10}$$

The continuity equation (1) is satisfied identically and (2), (4), and (6) yield

$$\begin{aligned} G_1 = {} & \frac{\partial\psi}{\partial y}\frac{\partial^2\psi}{\partial x\partial y} - \frac{\partial\psi}{\partial x}\frac{\partial^2\psi}{\partial y^2} - \left[1 + \zeta(1-\theta)\right]\frac{\partial^3\psi}{\partial y^3} \\ & + \zeta\frac{\partial\theta}{\partial y}\frac{\partial^2\psi}{\partial y^2} + M^* B_0^2(x)\frac{\partial\psi}{\partial y} = 0 \end{aligned} \tag{11}$$

$$\begin{aligned} G_2 = {} & \frac{\partial\psi}{\partial y}\frac{\partial\theta}{\partial x} - \frac{\partial\psi}{\partial x}\frac{\partial\theta}{\partial y} \\ & - \frac{1}{\mathrm{Pr}}\left(1 + \frac{4R}{3}\right)\frac{\partial^2\theta}{\partial y^2} - \gamma^* Q_0(x)\theta = 0, \end{aligned} \tag{12}$$

$$\begin{aligned} G_3 = {} & \frac{\partial\psi}{\partial y}\frac{\partial\phi}{\partial x} - \frac{\partial\psi}{\partial x}\frac{\partial\phi}{\partial y} - \frac{1}{\mathrm{Sc}}\left(1 + n\phi\right)\frac{\partial^2\phi}{\partial y^2} \\ & - \frac{n}{\mathrm{Sc}}\left(\frac{\partial\phi}{\partial y}\right)^2 + \alpha^* K(x)\phi = 0. \end{aligned} \tag{13}$$

The boundary conditions (5) now become

$$\begin{aligned} \frac{\partial\psi}{\partial y} &= U_w(x) + \lambda^*\lambda_0(x)\left[1 + \zeta(1-\theta)\right]\frac{\partial^2\psi}{\partial y^2}, \\ \frac{\partial\psi}{\partial x} &= V^* V_w(x), \\ \frac{\partial\theta}{\partial y} &= -h^* h_f(x)[1-\theta], \qquad \phi = 1, \quad \text{at } y = 0, \end{aligned} \tag{14}$$

$$\frac{\partial\psi}{\partial y} \longrightarrow 0, \qquad \theta \longrightarrow 0, \qquad \phi \longrightarrow 0, \quad \text{as } y \longrightarrow \infty, \tag{15}$$

where $\zeta = b_0(\overline{T}_f - \overline{T}_\infty)$, $n = d(\overline{C}_w - \overline{C}_\infty)$, $M^* = \sigma_0 L/\rho U_0$, $\gamma^* = L/\rho c_p U_0$, $\lambda^* = \mu_\infty\sqrt{\mathrm{Re}}/L$, $V^* = 1/\sqrt{\mathrm{Re}}$, $h^* = L/\kappa U_0\sqrt{\mathrm{Re}}$, $R = 4\sigma_1\overline{T}_\infty^3/\kappa\kappa^*$, $\mathrm{Sc} = \nu/D_m$, $\mathrm{Pr} = \rho\nu Cp/\kappa$, and $\alpha^* = L/U_0$. The quantities Pr, ζ, n, R, and Sc are the Prandtl number, the viscosity parameter, the concentration diffusivity parameter, the radiation parameter, and the Schmidt number, respectively.

3. Symmetries of the Problem

In this section, we apply the Lie group of transformations which leaves the equations (11)–(13) invariant. Firstly, we consider Lie group of transformations with independent variables x and y and dependent variables ψ, Θ, and Φ for the problem

$$\begin{aligned} x^* &= x^*(x, y, \psi, \theta, \phi; \varepsilon), \\ y^* &= y^*(x, y, \psi, \theta, \phi; \varepsilon), \\ \psi^* &= \psi^*(x, y, \psi, \theta, \phi; \varepsilon), \\ \Theta^* &= \Theta^*(x, y, \psi, \theta, \phi; \varepsilon), \\ \Phi^* &= \Phi^*(x, y, \psi, \theta, \phi; \varepsilon), \end{aligned} \tag{16}$$

where ε is the group parameter. The infinitesimal generator of the group (16) can be expressed in the following vector form:

$$\Gamma = X\frac{\partial}{\partial x} + Y\frac{\partial}{\partial y} + \Psi\frac{\partial}{\partial \psi} + \Theta\frac{\partial}{\partial \theta} + \Phi\frac{\partial}{\partial \phi}, \tag{17}$$

in which X, Y, Ψ, Θ, and Φ are infinitesimal functions of the group variables. Then, the corresponding one-parameter Lie group of transformations is given by

$$\begin{aligned} x^* &= e^{\varepsilon\chi}(x) = x + \varepsilon X(x, y, \psi, \theta, \phi) + O\left(\varepsilon^2\right), \\ y^* &= e^{\varepsilon\chi}(y) = y + \varepsilon Y(x, y, \psi, \theta, \phi) + O\left(\varepsilon^2\right), \\ \psi^* &= e^{\varepsilon\chi}(\psi) = \psi + \varepsilon\Psi(x, y, \psi, \theta, \phi) + O\left(\varepsilon^2\right), \\ \Theta^* &= e^{\varepsilon\chi}(\theta) = \Theta + \varepsilon\Theta(x, y, \psi, \theta, \phi) + O\left(\varepsilon^2\right), \\ \Phi^* &= e^{\varepsilon\chi}(\phi) = \Phi + \varepsilon\Phi(x, y, \psi, \theta, \phi) + O\left(\varepsilon^2\right). \end{aligned} \tag{18}$$

The action of the infinitesimal generator Γ is extended to all derivatives appearing in equations (11)–(13) through the third prolongation

$$\begin{aligned} \Gamma^{(3)} = \Gamma &+ \Psi^{[x]}\frac{\partial}{\partial \psi_x} + \Psi^{[y]}\frac{\partial}{\partial \psi_y} \\ &+ \Theta^{[x]}\frac{\partial}{\partial \theta_x} + \Theta^{[y]}\frac{\partial}{\partial \theta_x} + \Phi^{[x]}\frac{\partial}{\partial \phi_x} \\ &+ \Phi^{[y]}\frac{\partial}{\partial \phi_y} + \eta_1^{(xy)}\frac{\partial}{\partial \psi_{xy}} + \Psi^{[yy]}\frac{\partial}{\partial \psi_{yy}} \\ &+ \Theta^{[yy]}\frac{\partial}{\partial \theta_{yy}} + \Phi^{[yy]}\frac{\partial}{\partial \phi_{yy}} + \Psi^{[yyy]}\frac{\partial}{\partial \psi_{yyy}}, \end{aligned} \tag{19}$$

where $\Psi^{[x]}, \Psi^{[y]}, \Theta^{[x]}, \ldots, \Psi^{[yyy]}$ are the infinitesimal functions corresponding the derivatives. The infinitesimal generator Γ is a point symmetry of (11)-(12) if

$$\Gamma^{(3)}(G_i)\big|_{G_{i=0}} = 0, \quad i = 1, 2\ 3. \tag{20}$$

Since the coefficients of Γ do not involve derivatives, we can separate (20) with respect to derivatives and solve the result over a determined system of linear homogeneous partial differential equations known as the determining equations. After straightforward calculations for the determining equations, we find the solutions X, Y, Ψ, Θ, and Φ of the determining equations in the form

$$\begin{aligned} X &= (c_1 - c_2)x - c_3, \qquad Y = -c_2 y + g(x), \\ \Psi &= c_4 + c_2\psi, \qquad \Theta = \Phi = 0, \end{aligned} \tag{21}$$

where c_j $(j = 1, 2, 3, 4)$ are arbitrary constants and $g(x)$ is the infinite parameter Lie group transformation, and the functions satisfy the following ordinary differential equations:

$$[(c_1 - c_2)x + c_3]\frac{dB_0(x)}{dx} - c_2 B_0(x) = 0, \tag{22}$$

$$[(c_1 - c_2)x + c_3]\frac{dQ(x)}{dx} - 2c_2 Q(x) = 0, \tag{23}$$

$$[(c_1 - c_2)x + c_3]\frac{dK(x)}{dx} - 2c_2 K(x) = 0, \tag{24}$$

which directly give the form for the functions $B(x)$, $Q(x)$, and $K(x)$,

$$\begin{aligned} B(x) &= A_1\left(x + \frac{c_3}{c_1 - c_2}\right)^{c_2/(c_1 - c_2)}, \\ Q_0(x) &= A_2\left(x + \frac{c_3}{c_1 - c_2}\right)^{2c_2/(c_1 - c_2)}, \\ K(x) &= A_3\left(x + \frac{c_3}{c_1 - c_2}\right)^{2c_2/(c_1 - c_2)}, \end{aligned} \tag{25}$$

where A_1, A_2, and A_3 are arbitrary constants and $c_1 \neq c_2$.

Imposing the restrictions from boundaries and from the boundary conditions on the infinitesimals, we obtain $g(x) = c_4 = 0$.

What remains is to require invariance of the data which must be held on the boundary surface. This requirement means

$$\begin{aligned} &\Gamma^{(2)}\left[\psi_y - U_w(x) - \lambda^*\lambda_0(x)\left[1 + \zeta(1 - \theta)\right]\psi_{yy}\right] = 0, \\ &\text{when } \psi_y(x, 0) = U_w(x) + \lambda^*\lambda_0(x)\left[1 + \zeta(1 - \theta(x, 0))\right] \\ &\qquad \times \psi_{yy}(x, 0), \\ &\Gamma^{(1)}\left[\psi_x - V^* V_w(x)\right] = 0, \quad \text{when } \psi_x(x, 0) = V^* V_w(x), \\ &\Gamma^{(1)}\left[\theta_y + h^* h_f(x)\left[1 - \theta\right]\right] = 0, \\ &\text{when } \theta_y(x, 0) = -h^* h_f(x)\left[1 - \theta\right]. \end{aligned} \tag{26}$$

Examining the aforementioned conditions, we obtain the following differential equations:

$$\begin{aligned} &[(c_1 - c_2)x + c_3]\frac{d\lambda_0(x)}{dx} - c_2\lambda_0(x) = 0, \\ &[(c_1 - c_2)x + c_3]\frac{dU_w(x)}{dx} - (c_1 + c_2)U_w(x) = 0, \\ &[(c_1 - c_2)x + c_3]\frac{dV_w(x)}{dx} - c_2 V_w(x) = 0, \\ &[(c_1 - c_2)x + c_3]\frac{dh_f(x)}{dx} - c_2 h_f(x) = 0, \end{aligned} \tag{27}$$

which have the following solutions:

$$U_w(x) = A_4\left(x + \frac{c_3}{c_1 - c_2}\right)^{(c_1+c_2)/(c_1-c_2)},$$
$$\lambda_0(x) = A_5\left(x + \frac{c_3}{c_1 - c_2}\right)^{-c_2/(c_1-c_2)},$$
$$V_w(x) = A_6\left(x + \frac{c_3}{c_1 - c_2}\right)^{c_2/(c_1-c_2)}, \quad (28)$$
$$h_f(x) = A_7\left(x + \frac{c_3}{c_1 - c_2}\right)^{c_2/(c_1-c_2)},$$

where A_4, A_5, A_6, and A_7 are arbitrary constants.

Having determined the infinitesimals X, Y, Ψ, Θ, and Φ, the similarity variables are found by solving the characteristic equations

$$\frac{dx}{(c_1 - c_2)x + c_3} = \frac{dy}{-c_1 y} = \frac{d\psi}{c_1\psi} = \frac{d\theta}{0} = \frac{d\phi}{0}. \quad (29)$$

Solving (29), we have the following similarity transformations (absolute invariants):

$$\eta = y\left(x + \frac{c_3}{c_1 - c_2}\right)^{c_2/(c_1-c_2)},$$
$$\psi = \left(x + \frac{c_3}{c_1 - c_2}\right)^{c_1/(c_1-c_2)} f(\eta), \quad (30)$$
$$\theta = \theta(\eta), \qquad \phi = \varphi(\eta).$$

Substituting the transformation (30) into (11)–(15) yields the following nonlinear system of ordinary differential equations for $f(\eta)$, $\theta(\eta)$, and $\varphi(\eta)$:

$$(1 + \zeta(1 - \theta))f''' + \frac{c_1}{c_1 - c_2}ff'' - \frac{c_1 + c_2}{c_1 - c_2}f'^2 - \zeta\theta' f'' - Mf' = 0,$$
$$\left(1 + \frac{4R}{3}\right)\theta'' + \Pr\left(\frac{c_1}{c_1 - c_2}f\theta' + Q\theta\right) = 0, \quad (31)$$
$$\frac{1}{\mathrm{Sc}}(1 + n\varphi)\varphi'' + \frac{c_1}{c_1 - c_2}f\varphi' + \frac{n}{\mathrm{Sc}}\varphi'^2 - K_0\varphi = 0.$$

The boundary conditions now become

$$f' = 1 + \lambda[1 + \zeta(1 - \theta)]f'',$$
$$f = f_w, \quad \theta' = -\gamma[1 - \theta], \quad \varphi' = 1, \quad \text{at } \eta = 0, \quad (32)$$
$$f' = 0, \qquad \theta = 0, \qquad \varphi = 0, \qquad \text{as } \eta \longrightarrow \infty,$$

where $Q = \gamma^* A_2$ is the heat generation/absorption parameter, $M = A_1 M^*$ is the magnetic parameter, $K_0 = \alpha^* A_3$ is the chemical reaction parameter, $\lambda = \lambda^* A_5$ is the slip parameter, $\gamma = h^* A_7$ is the Boit number, and $f_w = V^* A_6$ is the suction/injection parameter and $A_4 = 1$.

Table 1: Comparison of skin friction coefficient $-f''(0)$ for various values of slip parameter λ when $\zeta = R = M = R = M = Q = K_0 = c_2 = c_3 = f_w = 0$, and $\gamma \to \infty$.

λ	Hayat et al. [21]	Hamad et al. [24]	Present work
0	1	1	1
0.1	0.87208247	0.87208247	0.87208247
0.2	0.776377	0.77637707	0.776377
0.5	0.591195	0.59119548	0.591195
1	0.430162	0.43015970	0.430162
2	0.283981	0.28397959	0.283981
5	0.144841	0.14484019	0.14484
10	0.081249	0.08124198	0.081249
20	0.043782	0.04378834	0.043782
50	0.018634	0.01859623	0.018634
100	0.009581	0.00954997	0.009581

3.1. Particular Cases

(i) For $\zeta = R = M = Q = K_0 = c_2 = c_3 = 0$, (3) and boundary conditions (32) reduce to (23)–(25) and boundary conditions (26) of Hamad [24].

(ii) For $\zeta = n = Q = K_0 = M = c_3 = \lambda = 0$ and $c_2 = (-1/2)c_1$, (31) and boundary conditions (32) reduce to (17)–(19) and boundary conditions (20) of Ferdows [44] when $G_r = G_c = m = M = 0$.

3.2. Physical Quantities of Interest. The parameters in which we are interested for our problem are the local skin friction coefficient f_x, the local Nusselt number Nu_x, and the local Sherwood number Sh_x, which are defined, respectively, as

$$\frac{1}{2}Cf_x(\mathrm{Re}_x)^{1/2} = -(1 + \zeta\theta(0))f''(0),$$
$$\mathrm{Nu}_x(\mathrm{Re}_x)^{-1/2} = -\theta'(0), \quad (33)$$
$$\mathrm{Sh}_x(\mathrm{Re}_x)^{-1/2} = -\varphi'(0),$$

where $\mathrm{Re}_x = (\overline{xu}/\nu)$ indicates the local Reynolds number.

4. Numerical Solution and Discussion

The transformed system of nonlinear ordinary differential equations (31) with the boundary conditions (32) has been solved numerically by using a fourth-order Runge-Kutta integration along with shooting techniques. In order to verify the accuracy of our results, we have compared the computed values of $-f''(0)$ with the previously published works by Hamad et al. [24], and Hayat et al. [21] with $f_w = 0$ and $\gamma \to \infty$ at different values of λ as shown in Table 1. The results of $-f''(0)$, $-\theta'(0)$ and $-\varphi'(0)$ for $\Pr = 0.72$, $\mathrm{Sc} = 0.22$, $n = 0.2$, $\gamma = 0.5$, and $f_w = -0.5$ for various values of λ are compared with those obtained by Hamad et al. [24] and are listed in Table 2. Moreover, Table 3 represents the comparison of $-\varphi'(0)$ between our results and the results obtained by Hamad et al. [24] for $\Pr = 0.72$, $\lambda = 0.2$, $\gamma = 0.5$,

Table 2: Comparison of values of $-f''(0)$, $-\theta'(0)$, and $-\varphi'(0)$ for $\zeta = R = M = R = M = Q = K_0 = c_2 = c_3 = 0$, Pr = 0.72, $f_w = -0.5$, Sc = 0.22, $n = 0.2$, $\gamma = 0.5$, and $\eta_{\max} = 20$.

λ	$-f''(0)$		$-\theta'(0)$		$-\varphi'(0)$	
	Hamad et al. [24]	Present work	Hamad et al. [24]	Present work	Hamad et al. [24]	Present work
0	0.78077641159	0.780776	0.1738614482	0.173859	0.1148467203	0.1148467
0.5	0.4925323862	0.492532	0.1478033629	0.147789	0.0972062425	0.0972061
1	0.3683505453	0.368350	0.1317723331	0.131737	0.0878003658	0.0878003
1.5	0.2969706178	0.296970	0.1201962831	0.120196	0.0815754873	0.0815754

Table 3: Values of $-\varphi'(0)$ for $\zeta = R = M = R = M = Q = K_0 = c_2 = c_3 = 0$, Pr = 0.72, $f_w = 0.5$, $\lambda = 0.2$, $\gamma = 0.5$, and $\eta_{\max} = 20$.

n	Sc = 0.22		Sc = 0.78	
	Hamad et al. [24]	Present work	Hamad et al. [24]	Present work
0	0.2357864723	0.235787	0.7103150065	0.710316
0.5	0.1622076843	0.162208	0.4969259049	0.496926
1	0.1243641685	0.124365	0.3857860094	0.385787
1.5	0.1013742450	0.101374	0.3166941114	0.316694

Table 4: Values of $-f''(0)$ for various values of f_w for $\zeta = n = Q = K_0 = c_3 = \lambda = 0$, $c_2 = (-1/2)c_1$, and $M = 0$.

f_w	Cortell [12]	Ferdows et al. [44]	Present work
−0.75	0.453521	0.453523	0.453523
−0.5	0.518869	0.518869	0.51887
0	0.677647	0.677648	0.677648
0.5	0.873627	0.873643	0.87363
0.75	0.984417	0.984439	0.98444

and $f_w = 0.5$ for various values of n. Also, the numerical results of $-f''(0)$ have been compared with those obtained by Ferdows et al. [44] for $M = 0$ at different values of f_w as shown in Table 4. In all comparisons, it is found that our results are in excellent agreement with the previous published results. Further, the values of the local skin friction, the local Nusselt number, and the local Sherwood number for different values of γ, K_0, Q, λ, M, and ζ are listed in Table 5. It is noted from this table that the local skin friction increases with increasing ζ, heat absorption ($Q < 0$), and M, while it decreases by increasing γ, λ, and heat generation ($Q > 0$). The local Nusselt number decreases with the increase of λ, M and heat generation ($Q > 0$), while the local Nusselt number increases with the increase of ζ, heat absorption ($Q < 0$), and γ. The local Sherwood number increases with the increase of ζ, heat absorption ($Q < 0$), and K_0, while it decreases with the increasing of γ, λ, M, and heat generation ($Q > 0$).

The profiles for velocity, temperature and concentration are shown in Figures 2–23, respectively, with various values of the parameters. Figures 2, 3, and 4 show the dimensionless velocity profiles $f'(\eta)$, the dimensionless temperature profiles and the dimensionless mass profiles in the boundary layer for various values of the viscosity parameter ζ. These figures depict that increase in the value of ζ the dimensionless velocity decreases near the surface but increases as larger distances, while the dimensionless temperature and the dimensionless mass in the boundary layer region decrease as the viscosity parameter increases.

Figures 5–7 exhibit the effect of the suction or injection parameter f_w on the dimensionless velocity profiles, the dimensionless temperature, and the dimensionless mass profiles. It is shown from Figure 5 that the suction parameter decreases the velocity indicating the usual fact that suction stabilizes the boundary layer growth, while injection increases the velocity in the boundary layer region indicating that injection helps the flow penetrate more into the fluid. In Figure 6, it is found that the temperature decreases as the suction parameter increases. This means that larger suction leads to faster cooling of the plate, while the temperature increases as the injection parameter increases; this is because of the heat transfer from fluid to surface. Figure 7 illustrates that the mass decreases as the suction parameter increases and increases as the injection parameter increases.

The dimensionless velocity profiles for different values of the Boit number γ are described in Figure 8. From this figure, we observe that an increase in γ leads to increase in f' near the wall but it decreases with larger distances, while Figure 9 shows that the dimensionless temperature decreases as the Boit number γ increases.

Effect of the chemical reaction parameter K_0 on the dimensionless concentration profiles is shown in Figure 10. It is seen that the dimensionless concentration of the fluid decreases with the increase of K_0.

Figures 11, 12, and 13 illustrate the influence of slip velocity parameter λ on the velocity, temperature, and concentration profiles, respectively. It is obvious that slip parameter decreases the velocity f' and increases both dimensionless temperature θ and the dimensionless concentration φ.

Figures 14, 15, and 16 show the velocity, temperature, and concentration distributions for various values of the magnetic field M. We can notice that increasing M decreases the velocity f' and increases the temperature θ and concentration; this result qualitatively agrees with the expectations; this is because the application of a transverse magnetic field to an electrically conducting fluid gives rise to a resistive-type force called the Lorentz force. This force has the tendency to slow down the motion of the fluid in the boundary layer and to increase its temperature and concentration.

Figure 17 illustrates the effect of the concentration diffusivity parameter n on the concentration profiles; one can observe that the concentration profiles increase as n increases.

The effects of the Prandtl number Pr on the dimensionless velocity and temperature dimensionless velocity are

Table 5: Values of $(-1/2)Cf_x(\mathrm{Re}_x)^{1/2}$, $-\mathrm{Nu}_x(\mathrm{Re}_x)^{-1/2}$, and $-\mathrm{Sh}_x(\mathrm{Re}_x)^{-1/2}$ for $f_w = 0.5$, Pr = 0.72, Sc = 0.6, $n = 0.5$, and $R = 1$.

ζ	K_0	γ	λ	M	Q	$(-1/2)Cf_x(\mathrm{Re}_x)^{1/2}$	$-\mathrm{Nu}_x(\mathrm{Re}_x)^{-1/2}$	$-\mathrm{Sh}_x(\mathrm{Re}_x)^{-1/2}$
0	0.01	1	0.3	0.5	−0.2	0.8282097	0.267065009	0.2817571148
2	0.01	1	0.3	0.5	−0.2	0.98684111	0.272061144	0.30316651
5	0.01	1	0.3	0.5	−0.2	1.16050976	0.275202928	0.31591854
0.1	0	1	0.3	0.7	−0.5	0.89348981	0.329592869	0.263842318
0.1	1	1	0.3	0.7	−0.5	0.89348981	0.329592869	0.70701644
0.1	3	1	0.3	0.7	−0.5	0.89348981	0.329592869	1.128126581
1	0.3	0.1	0.3	0.5	−0.2	0.9886912570	0.07894766720	0.4729295509
1	0.3	0.5	0.3	0.5	−0.2	0.938324634	0.213201753	0.46994994
1	0.3	1	0.3	0.5	−0.2	0.913264332	0.270045367	0.468340615
0.1	0.5	0.1	0	0.7	−0.2	1.29926459	0.079169100	0.56364235
0.1	0.5	0.1	1	0.7	−0.2	0.53978525	0.077353309	0.52577635
0.1	0.5	0.1	2	0.7	−0.2	0.34699071054	0.07673167148	0.5143743566
0.1	0.6	0.7	0.5	0	−1	0.5697224247	0.08671881627	0.5920198931
0.1	0.6	0.7	0.5	1	−1	0.80801328749	0.08644826115	0.5705347139
0.1	0.6	0.7	0.5	3	−1	1.0116231621	0.08626331255	0.5563999142
0.7	0.5	0.8	1	0.5	−0.8	0.5409262133	0.335939548322	0.52997592226
0.7	0.5	0.8	1	0.5	−0.3	0.535413351	0.265641294131	0.52980646921
0.7	0.5	0.8	1	0.5	0	0.5252295045	0.15291844567	0.529531543678
0.7	0.5	0.8	1	0.5	0.02	0.52331016216	0.13341074189	0.52948110939
0.7	0.5	0.8	1	0.5	0.1	0.51234845001	0.037287564758	0.52938666933

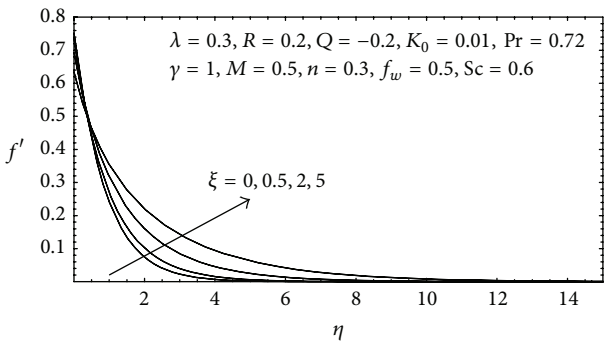

Figure 2: Velocity distribution for various values of ζ.

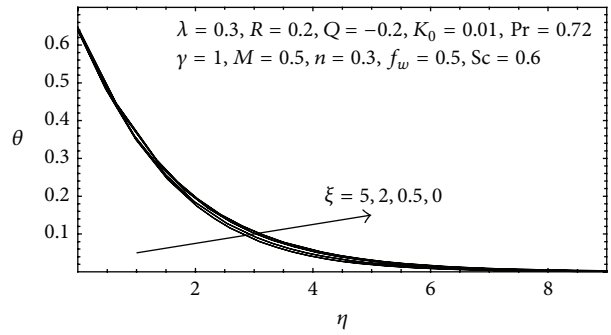

Figure 3: Temperature distribution for various values of ζ.

illustrated in Figures 18 and 19, respectively. From Figure 18, it can be seen that as the Prandtl number Pr increases, the dimensionless velocity decreases near the surface but increases with larger distances. Figure 19 illustrates that the dimensionless temperature decreases with increasing Pr; this is because, when the Prandtl number increases the thickness of the thermal boundary layer decreases and, hence, the temperature decreases.

The effects of the presence of heat source ($Q > 0$) or heat sink ($Q < 0$) in the boundary layer on the velocity and temperature profiles are presented in Figures 20 and 21, respectively. From Figure 20, one sees that the dimensionless velocity decreases with the heat source ($Q > 0$) increasing, while it increases with the heat sink ($Q < 0$) increasing. The presence of heat source in the boundary layer generates energy which causes the temperature of the fluid to increase. On the other hand, the presence of heat sink in the boundary layer absorbs energy which causes the temperature of the fluid to decrease, and this corresponds with the observation in Figure 21, in which we note that the dimensionless temperature increases with the heat source ($Q > 0$) increasing, while it decreases with the heat sink ($Q < 0$) increasing.

For different values of radiation parameter R, the dimensionless velocity profiles are plotted in Figure 22. It is obvious that velocity decreases with the increase in R. The effects on the temperature profiles are presented in Figure 23. From this figure, we observed that, as the value of R increases, the temperature profiles increase, with an increase in the thermal boundary layer thickness.

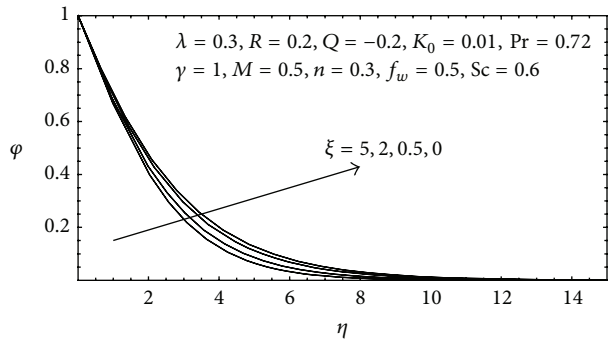

Figure 4: Mass distribution for various values of ζ.

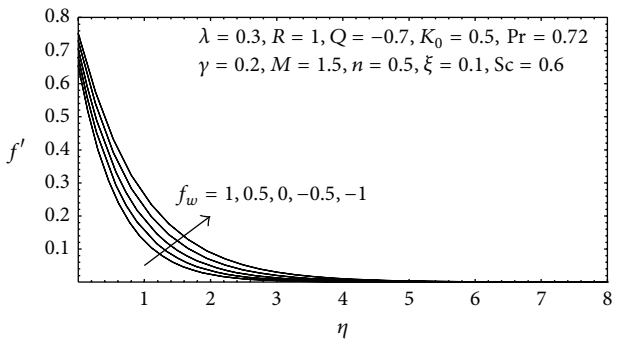

Figure 5: Velocity distribution for various values of f_w.

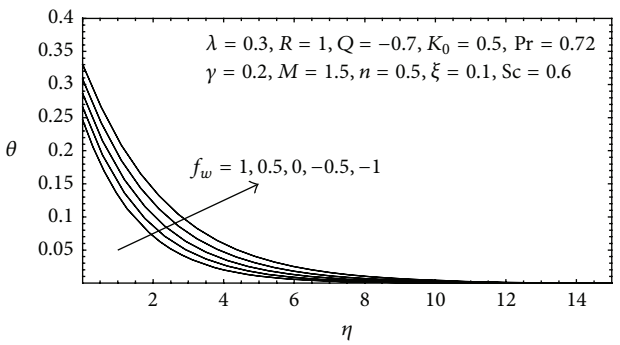

Figure 6: Temperature distribution for various values of f_w.

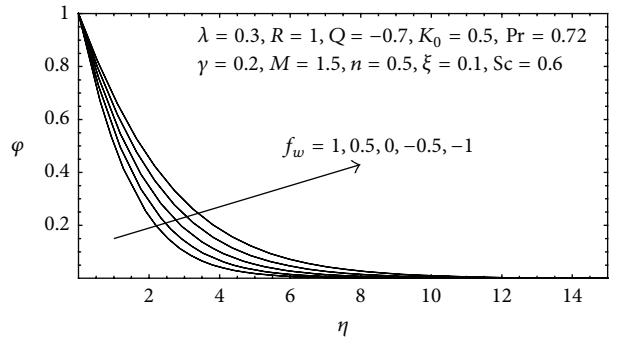

Figure 7: Mass distribution for various values of f_w.

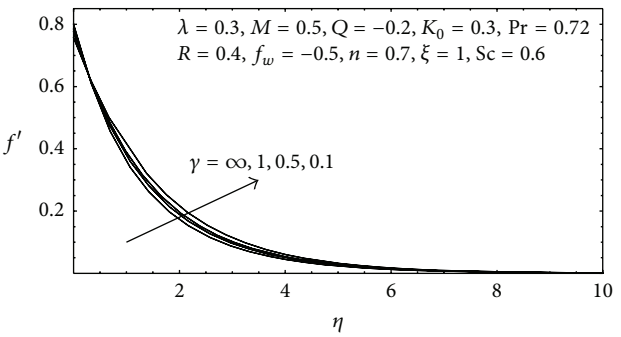

Figure 8: Velocity distribution for various values of γ.

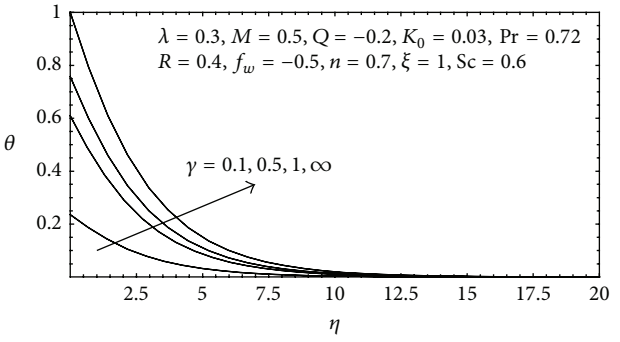

Figure 9: Temperature distribution for various values of γ.

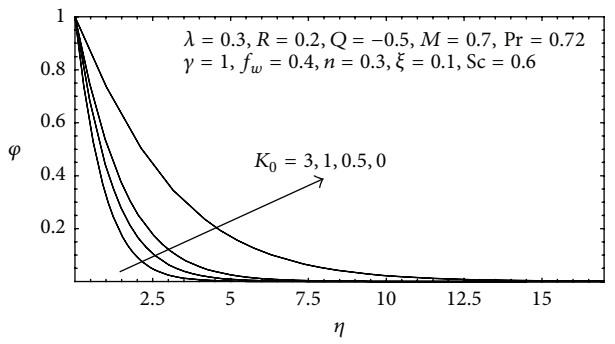

Figure 10: Mass distribution for various values of K_0.

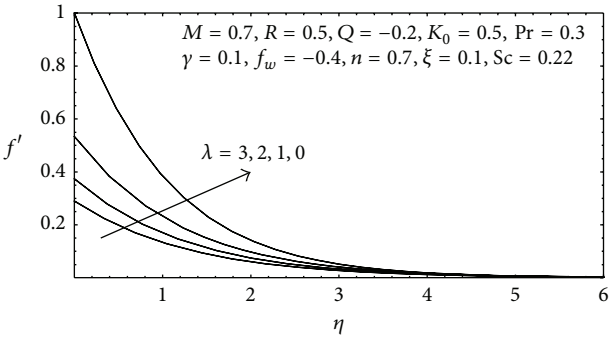

Figure 11: Velocity distribution for various values of λ.

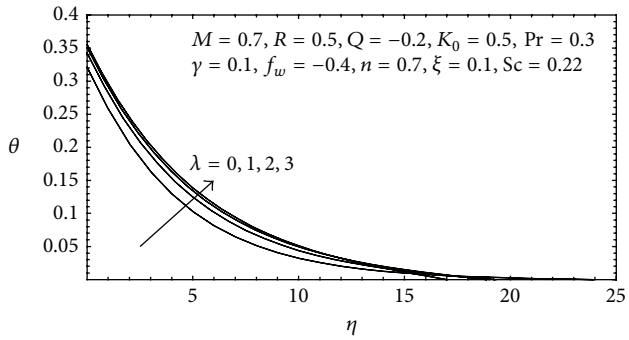

Figure 12: Temperature distribution for various values of λ.

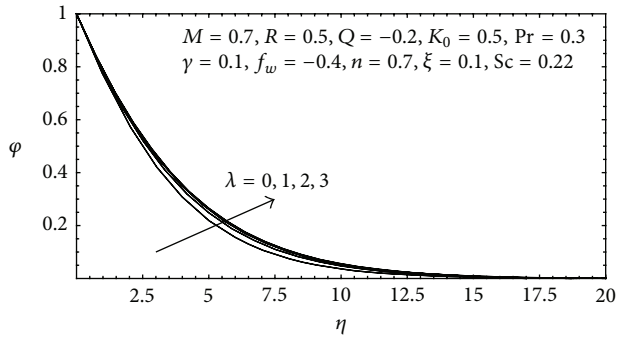

Figure 13: Mass distribution for various values of λ.

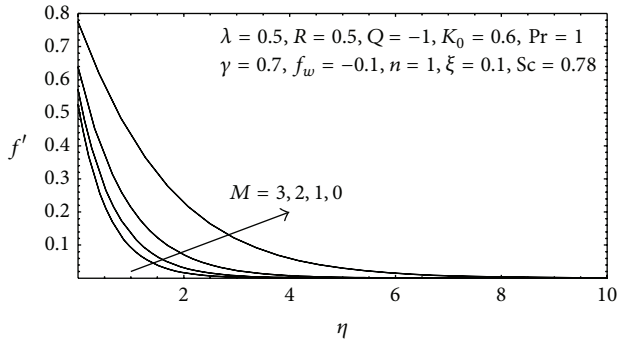

Figure 14: Velocity distribution for various values of M.

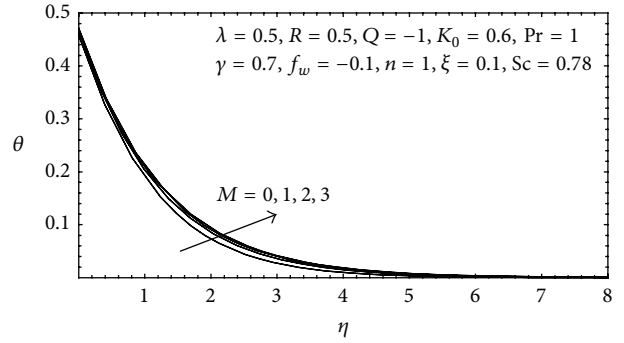

Figure 15: Temperature distribution for various values of M.

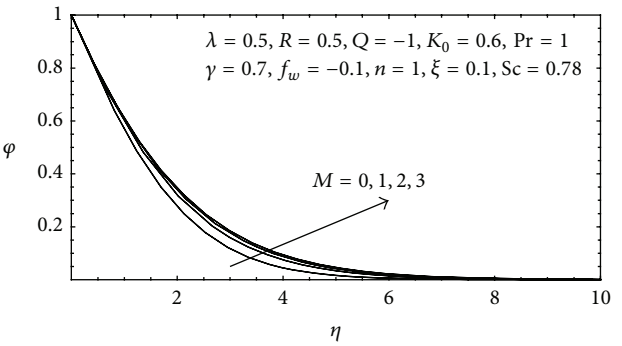

Figure 16: Mass distribution for various values of M.

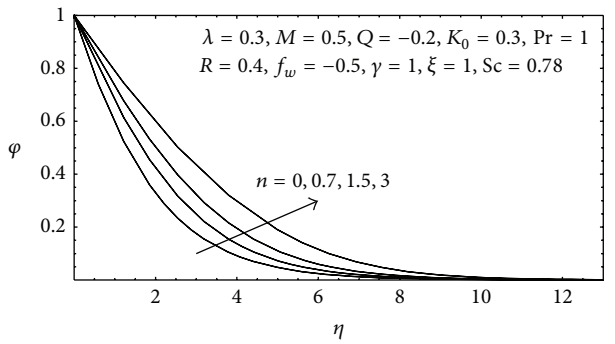

Figure 17: Mass distribution for various values of n.

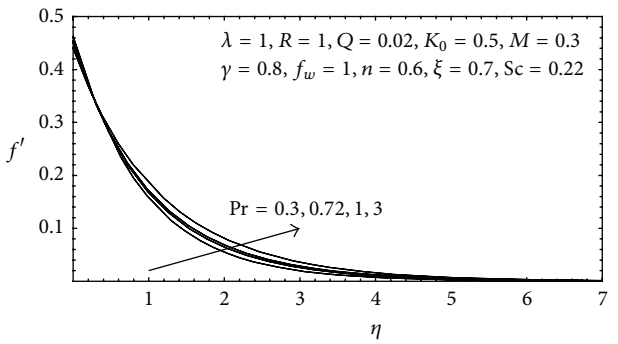

Figure 18: Velocity distribution for various values of Pr.

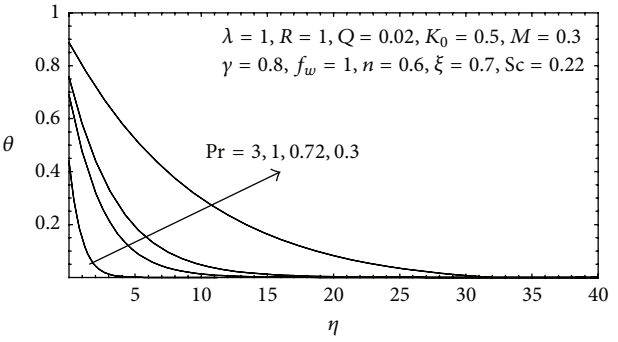

Figure 19: Temperature distribution for various values of Pr.

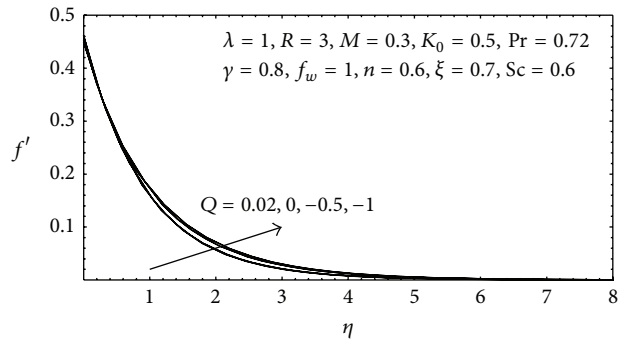

Figure 20: Velocity distribution for various values of Q.

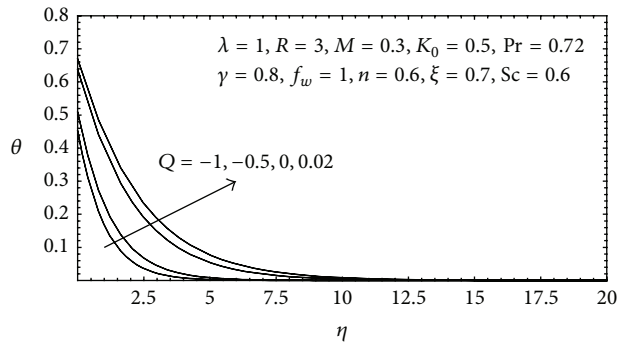

Figure 21: Temperature distribution for various values of Q.

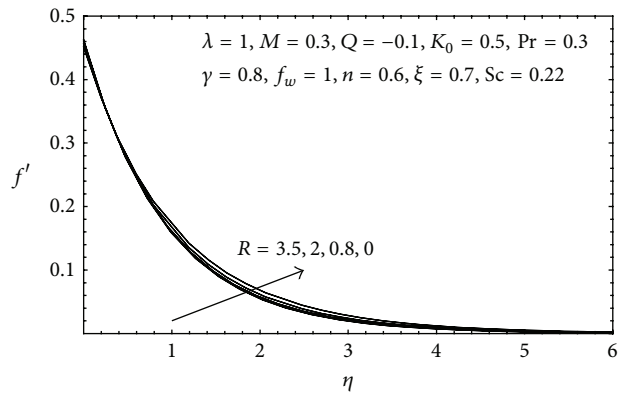

Figure 22: Velocity distribution for various values of R.

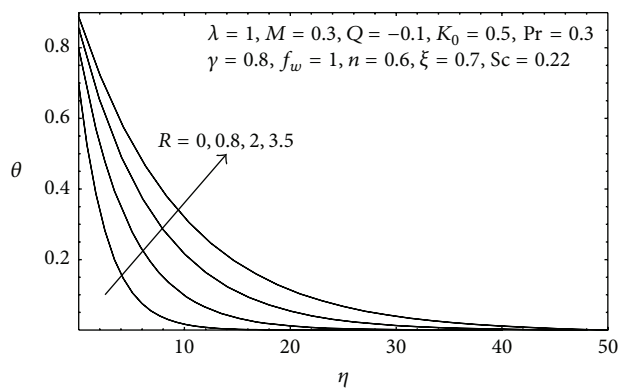

Figure 23: Temperature distribution for various values of R.

5. Conclusions

In this study, the symmetries of the problem of heat and mass transfer flow over a moving permeable flat stretching sheet in the presence of thermal radiation, variable viscosity, a uniform transverse magnetic field, chemical reaction, heat generation/absorption, suction/injection, convective boundary condition, and slip velocity are obtained using Lie group analysis. Numerical solutions of the resulting system of nonlinear ordinary differential equations are obtained by using the shooting method coupled with Runge-Kutta scheme. The effects of various parameters on the dimensionless velocity, temperature, and concentration profiles have been studied graphically. The influence of some parameters on the local skin friction, local Nusselt number, and local Sherwood number is tabulated. It was found that with the increase of the convective parameter n, injection parameter $f_w < 0$, and the slip velocity λ, the absolute concentration increases, while it decreases with the increase in the magnetic parameter M, viscosity parameter ζ, suction parameter $f_w > 0$, and chemical reaction parameter K_0.

References

[1] B. C. Sakiadis, "Boundary-Layer behavior on continuous solid surfaces: I. Boundary layer equations for two-dimensional and axisymmetric flow," *AIChE Journal*, vol. 7, pp. 26–28, 1961.

[2] V. G. Fox, L. E. Erickson, and L. T. Fan, "Methods for solving the boundary layer equations for moving continuous flat surfaces with suction and injection," *AIChE Journal*, vol. 14, pp. 726–736, 1968.

[3] P. S. Gupta and A. S. Gupta, "Heat transfer of a continuous stretching surface with suction or blowing," *The Canadian Journal of Chemical Engineering*, vol. 55, pp. 744–746, 1977.

[4] V. M. Soundalgekar and T. V. R. Murty, "Heat transfer in MHD flow with pressure gradient, suction and injection," *Journal of Engineering Mathematics*, vol. 14, no. 2, pp. 155–159, 1980.

[5] L. J. Grubka and K. M. Bobba, "Heat transfer characteristics of a continuous stretching surface with variable temperature," *Journal of Heat Transfer*, vol. 107, no. 1, pp. 248–250, 1985.

[6] B. K. Dutta, "Heat transfer from a stretching sheet with uniform suction and blowing," *Acta Mechanica*, vol. 78, no. 3-4, pp. 255–262, 1989.

[7] S. L. Lee and J. S. Tsai, "Cooling of a continuous moving sheet of finite thickness in the presence of natural convection," *International Journal of Heat and Mass Transfer*, vol. 33, no. 3, pp. 457–464, 1990.

[8] R. Cortell, "Flow and heat transfer in a moving fluid over a moving flat surface," *Theoretical and Computational Fluid Dynamics*, vol. 21, no. 6, pp. 435–446, 2007.

[9] R. Cortell, "Toward an understanding of the motion and mass transfer with chemically reactive species for two classes of viscoelastic fluid over a porous stretching sheet," *Chemical Engineering and Processing*, vol. 46, no. 10, pp. 982–989, 2007.

[10] T. Fang, "Flow and heat transfer characteristics of the boundary layers over a stretching surface with a uniform-shear free stream," *International Journal of Heat and Mass Transfer*, vol. 51, no. 9-10, pp. 2199–2213, 2008.

[11] M. A. A. Mahmoud, "Hydromagnetic stagnation point flow towards a porous stretching sheet with variable surface heat

flux in the presence of heat generation," *Chemical Engineering Communications*, vol. 198, no. 7, pp. 837–846, 2011.

[12] R. Cortell, "Heat and fluid flow due to non-linearly stretching surfaces," *Applied Mathematics and Computation*, vol. 217, no. 19, pp. 7564–7572, 2011.

[13] M. J. Martin and I. D. Boyd, "Momentum and heat transfer in a laminar boundary layer with slip flow," *Journal of Thermophysics and Heat Transfer*, vol. 20, no. 4, pp. 710–719, 2006.

[14] T. Fang and C.-F. F. Lee, "A moving-wall boundary layer flow of a slightly rarefied gas free stream over a moving flat plate," *Applied Mathematics Letters*, vol. 18, no. 5, pp. 487–495, 2005.

[15] P. D. Ariel, T. Hayat, and S. Asghar, "The flow of an elastico-viscous fluid past a stretching sheet with partial slip," *Acta Mechanica*, vol. 187, no. 1–4, pp. 29–35, 2006.

[16] H. I. Andersson, "Slip flow past a stretching surface," *Acta Mechanica*, vol. 158, no. 1-2, pp. 121–125, 2002.

[17] C. Y. Wang, "Stagnation slip flow and heat transfer on a moving plate," *Chemical Engineering Science*, vol. 61, no. 23, pp. 7668–7672, 2006.

[18] C. Y. Wang, "Analysis of viscous flow due to a stretching sheet with surface slip and suction," *Nonlinear Analysis: Real World Applications*, vol. 10, no. 1, pp. 375–380, 2009.

[19] S. Mukhopadhyay and H. I. Andersson, "Effects of slip and heat transfer analysis of flow over an unsteady stretching surface," *Heat and Mass Transfer*, vol. 45, no. 11, pp. 1447–1452, 2009.

[20] T. Fang, J. Zhang, and S. Yao, "Slip MHD viscous flow over a stretching sheet—an exact solution," *Communications in Nonlinear Science and Numerical Simulation*, vol. 14, no. 11, pp. 3731–3737, 2009.

[21] T. Hayat, M. Qasim, and S. Mesloub, "MHD flow and heat transfer over permeable stretching sheet with slip conditions," *International Journal for Numerical Methods in Fluids*, vol. 66, no. 8, pp. 963–975, 2011.

[22] T.-G. Fang, J. Zhang, and S.-S. Yao, "Slip magnetohydrodynamic viscous flow over a permeable shrinking sheet," *Chinese Physics Letters*, vol. 27, no. 12, Article ID 124702, 2010.

[23] M. Mahmoud and S. Waheed, "Effects of slip and heat generation/absorption on MHD mixed convection flow of a micropolar fluid over a heated stretching surface," *Mathematical Problems in Engineering*, vol. 2010, Article ID 579162, 20 pages, 2010.

[24] M. A. A. Hamad, M. J. Uddin, and A. I. M. Ismail, "Investigation of combined heat and mass transfer by Lie group analysis with variable diffusivity taking into account hydrodynamic slip and thermal convective boundary conditions," *International Journal of Heat and Mass Transfer*, vol. 55, no. 4, pp. 1355–1362, 2012.

[25] M. A. A. Mahmoud, "Thermal radiation effect on unsteady MHD free convection flow past a vertical plate with temperature-dependent viscosity," *Canadian Journal of Chemical Engineering*, vol. 87, no. 1, pp. 47–52, 2009.

[26] A. J. Chamkha, "Coupled heat and mass transfer by natural convection about a truncated cone in the presence of magnetic field and radiation effects," *Numerical Heat Transfer A*, vol. 39, no. 5, pp. 511–530, 2001.

[27] M. A. A. Mahmoud, "Variable viscosity effects on hydromagnetic boundary layer flow along a continuously moving vertical plate in the presence of radiation," *Applied Mathematical Sciences*, vol. 1, no. 17–20, pp. 799–814, 2007.

[28] R. Cortell, "Effects of viscous dissipation and radiation on the thermal boundary layer over a nonlinearly stretching sheet," *Physics Letters A*, vol. 372, no. 5, pp. 631–636, 2008.

[29] R. Cortell Bataller, "Radiation effects in the Blasius flow," *Applied Mathematics and Computation*, vol. 198, no. 1, pp. 333–338, 2008.

[30] T.-M. Chen, "Radiation effects on magnetohydrodynamic free convection flow," *Journal of Thermophysics and Heat Transfer*, vol. 22, no. 1, pp. 125–128, 2008.

[31] K.-L. Hsiao, "Mixed convection with radiation effect over a nonlinearly stretching sheet," *World Academy of Science, Engineering and Technology*, vol. 62, pp. 338–342, 2010.

[32] A. Ishak, N. A. Yacob, and N. Bachok, "Radiation effects on the thermal boundary layer flow over a moving plate with convective boundary condition," *Meccanica*, vol. 46, no. 4, pp. 795–801, 2011.

[33] R. N. Jet and S. Chaudhary, "Rediation effects on the MHD flow near the stagnation point of a nonlinearly stretching sheet," *Zeitschrift für Angewandte Mathematik und Physik*, vol. 33, pp. 2–5, 2010.

[34] A. J. Chamkha, "MHD flow of a uniformly streched vertical permeable surface in the presence of heat generation/absorption and a chemical reaction," *International Communications in Heat and Mass Transfer*, vol. 30, no. 3, pp. 413–422, 2003.

[35] A. J. Chamkha, "Unsteady MHD convective heat and mass transfer past a semi-infinite vertical permeable moving plate with heat absorption," *International Journal of Engineering Science*, vol. 42, no. 2, pp. 217–230, 2004.

[36] R. Cortell, "Flow and heat transfer of a fluid through a porous medium over a stretching surface with internal heat generation/absorption and suction/blowing," *Fluid Dynamics Research*, vol. 37, no. 4, pp. 231–245, 2005.

[37] R. Kandasamy, K. Periasamy, and K. K. Sivagnana Prabhu, "Chemical reaction, heat and mass transfer on MHD flow over a vertical stretching surface with heat source and thermal stratification effects," *International Journal of Heat and Mass Transfer*, vol. 48, no. 21-22, pp. 4557–4561, 2005.

[38] A. Raptis and C. Perdikis, "Viscous flow over a non-linearly stretching sheet in the presence of a chemical reaction and magnetic field," *International Journal of Non-Linear Mechanics*, vol. 41, no. 4, pp. 527–529, 2006.

[39] G. C. Layek, S. Mukhopadhyay, and S. A. Samad, "Heat and mass transfer analysis for boundary layer stagnation-point flow towards a heated porous stretching sheet with heat absorption/generation and suction/blowing," *International Communications in Heat and Mass Transfer*, vol. 34, no. 3, pp. 347–356, 2007.

[40] M. A. A. Mahmoud, "Soret effect on mixed convection heat and mass transfer along a semi-infinite horizontal plate in the presence of heat generation and chemical reaction," *Canadian Journal of Physics*, vol. 86, no. 11, pp. 1291–1296, 2008.

[41] A. Ishak, "Similarity solutions for flow and heat transfer over a permeable surface with convective boundary condition," *Applied Mathematics and Computation*, vol. 217, no. 2, pp. 837–842, 2010.

[42] O. D. Makinde, "On MHD heat and mass transfer over a moving vertical plate with a convective surface boundary condition," *Canadian Journal of Chemical Engineering*, vol. 88, no. 6, pp. 983–990, 2010.

[43] S. Yao, T. Fang, and Y. Zhong, "Heat transfer of a generalized stretching/shrinking wall problem with convective boundary conditions," *Communications in Nonlinear Science and Numerical Simulation*, vol. 16, no. 2, pp. 752–760, 2011.

[44] M. Ferdows, Md. J. Uddin, and A. A. Afify, "Scaling group transformation for MDH boundary layer free convective heat

and mass transfer flow past a convectively heated nonlinear radiating stretching sheet," *International Journal of Heat and Mass Transfer*, vol. 56, pp. 181–187, 2013.

[45] P. J. Olver, *Applications of Lie Groups to Differential Equations*, Springer, Berlin, Germany, 1986.

[46] G. W. Bluman and S. Kumei, *Symmetries and Differential Equations*, Springer, New York, NY, USA, 1989.

[47] J. M. Hill, *Differential Equations and Group Methods for Scientists and Engineers*, CRC Press, Boca Raton, Fla, USA, 1992.

[48] H. Ibragimov and V. F. Kovalev, *Approximate and Re-Norm Group Symmetry*, Springer, 2009.

[49] M. Pandey, B. D. Pandey, and V. D. Sharma, "Symmetry groups and similarity solutions for the system of equations for a viscous compressible fluid," *Applied Mathematics and Computation*, vol. 215, no. 2, pp. 681–685, 2009.

[50] R. Kandasamy, M. Ismoen, and H. B. Saim, "Lie group analysis for the effects of temperature-dependent fluid viscosity and chemical reaction on MHD free convective heat and mass transfer with variable stream conditions," *Nuclear Engineering and Design*, vol. 240, no. 1, pp. 39–46, 2010.

[51] P. Loganathan and P. Puvi Arasu, "Lie group analysis for the effects of variable fluid viscosity and thermal radiation on free convective heat and mass transfer with variable stream condition," *Engineering*, vol. 2, pp. 625–634, 2010.

[52] I. A. Hassanien, H. M. El-hawary, M. A. A. Mahmoud, R. G. Abdel -Rahman, and A. S. Elfeshawey, "Thermal radition effect on flow and heat transfer of unsteady MHD micropolar fluid over vertical heated non-isothermal stretching surface using group analysis," *Applied Mathematics and Mechanics*, vol. 34, no. 6, pp. 703–720, 2013.

[53] M. Q. Brewster, *Thermal Radiative Transfer and Properties*, John Wiley & Sons, New York, NY, USA, 1992.

[54] M. A. A. Hamad, M. J. Uddin, and A. I. M. Ismail, "Radiation effects on heat and mass transfer in MHD stagnation-point flow over a permeable flat plate with thermal convective surface boundary condition, temperature dependent viscosity and thermal conductivity," *Nuclear Engineering and Design*, vol. 242, pp. 194–200, 2012.

[55] R. E. White and V. R. Subramanian, *Computational Methods in Chemical Engineering With Maple*, Springer, 2010.